Kondo Effect in CeX_c (X_c=S, Se, Te) Studied by Electrical Resistivity Measurements under High Pressure

Yuya Hayashi[1], Shun Takai[1], Takeshi Matsumura[1,2], Hiroshi Tanida[1], Masafumi Sera[1,2], Kazuyuki Matsubayashi[3], Yoshiya Uwatoko[3], and Akira Ochiai[4]

[1]*Department of Quantum Matter, AdSM, Hiroshima University, Higashi-Hiroshima, Hiroshima 739-8530, Japan*
[2]*Institute for Advanced Materials Research, Hiroshima University, Higashi-Hiroshima, Hiroshima 739-8530, Japan*
[3]*Institute for Solid State Physics, University of Tokyo, Kashiwa, Chiba 277-8581, Japan*
[4]*Department of Physics, Graduate School of Science, Tohoku University, Sendai 980-8578, Japan*

We have measured the electrical resistivity of cerium monochalcogenides, CeS, CeSe, and CeTe, under high pressures of up to 8 GPa. The pressure dependences of the antiferromagnetic ordering temperature T_N, crystal field splitting, and the $\ln T$ anomaly of the Kondo effect have been studied to cover the entire region from the magnetic ordering regime at low pressure to the Fermi liquid regime at high pressure. T_N initially increases with increasing pressure, and starts to decrease at high pressure as expected from Doniach's diagram. Simultaneously, the $\ln T$ behavior in the resistivity is enhanced, indicating the enhancement of the Kondo effect by pressure. It is also characteristic of CeX_c that the crystal field splitting rapidly decreases at a common rate of -12.2 K/GPa. This leads to the increase in the degeneracy of the f state and the further enhancement of the Kondo effect. It is shown that the pressure-dependent degeneracy of the f state is a key factor for understanding the pressure dependence of T_N, the Kondo effect, magnetoresistance, and the peak structure in the temperature dependence of resistivity.

Journal Ref: J. Phys. Soc. Jpn., **85**, 034704 (2016).
http://dx.doi.org/10.7566/JPSJ.85.034704

1. Introduction

Through the hybridization between conduction electrons and the localized f state (c–f hybridization), f electrons at different atomic sites interact with each other, leading to a magnetic ordered state. This is the Ruderman–Kittel–Kasuya–Yosida (RKKY) interaction. At the same time, c–f hybridization causes the local spin and orbital degrees of freedom to be screened by conduction electrons, leading to the reduction in the local moment and magnetic ordering temperature. This is the Kondo effect. The strength of c–f hybridization, J_{cf}, is the primary parameter for describing these competing phenomena. In Ce-based compounds with one $4f$ electron, the RKKY interaction dominates the Kondo effect when J_{cf} is small, and the magnetic ordering temperature increases with increasing J_{cf}. With further increase in J_{cf}, the Kondo effect gradually dominates the RKKY interaction, and the magnetic ordering temperature starts to decrease. Finally, the magnetic ordering vanishes, and the c–f hybridized system forms a Fermi liquid ground state with a heavy effective mass. This general scheme has been described by Doniach's diagram.[1,2] Of particular interest in recent years is the critical region in the vicinity of J_{cf} where the magnetic ordering vanishes, which is called the quantum critical point (QCP). In this region, the order parameter fluctuation causes the physical properties to deviate from the Fermi liquid behavior, and in some cases causes unconventional superconductivity.[3–5] In the course of this study, the application of pressure is a suitable method of experimentally realizing the variation in J_{cf}.

CeS, CeSe, and CeTe, crystallizing in a cubic NaCl-type structure, exhibit antiferromagnetic (AFM) orderings with $\boldsymbol{q} = (\frac{1}{2}, \frac{1}{2}, \frac{1}{2})$ at T_N=8.4, 5.4, and 1.9 K, respectively.[6–8] In a cubic crystalline electric field (CEF), the Hund's rule ground multiplet of $J = 5/2$ splits into the Γ_7 doublet and Γ_8 quartet. It is already well established that the ground state of CeX_c is Γ_7 and that the energy level of the Γ_8 state is at 140, 116, and 32 K for CeS, CeSe, and CeTe, respectively.[9–11] The magnitudes of the ordered moments in the AFM phase are 0.57, 0.56, and 0.3 μ_B for CeS, CeSe, and CeTe, respectively. The reduction in the ordered moment from the expected value of 0.71 μ_B for the Γ_7 ground state can be ascribed to the Kondo effect. However, the largest reduction in CeTe cannot be explained by the Kondo effect only, because the Kondo effect is weakest in CeTe and strongest in CeS, as judged from the $\ln T$ anomaly ($d\rho/d\ln T$) in resistivity.[8] This remains an open question.

In most Ce-based compounds that have been studied to date under high pressure in the quantum critical region, the CEF ground states are well-isolated Kramers doublets, where only the magnetic dipolar degree of freedom plays a role. This is also the case in CeX_c at ambient pressure with the Γ_7 ground state. However, it has been strongly suggested by recent experiments on CeTe that the Γ_8 excited level decreases under high pressure.[12,13] CEF splitting is expected to vanish at approximately 2.5 GPa in CeTe. This means that the quadrupolar degree of freedom of the Γ_8 state also takes part in the physical properties at low temperatures. It has already been shown for CeTe that an antiferroquadrupolar interaction

through the Γ_8 excited level is essential for understanding the properties under high pressure.[13] Therefore, nontrivial phenomena could take place in the quantum critical region by an interplay between the nondipolar degrees of freedom and the Kondo effect. This is also an important issue in relation to the recent studies on Pr based compounds, where the role of quadrupolar fluctuation in the superconductivity attracts interest.[14] Studying CeX_c under high pressure, therefore, has its significance in investigating the possibility of multipolar degrees of freedom to participate in quantum critical phenomena.

Another advantage in studying CeX_c lies in its simple electronic structure. The localized f state hybridizes with the p-orbital of X_c, which forms a valence band. A conduction band is formed by the $5d$-orbital of Ce, containing one conduction electron per formula unit. The f level is located ~ 2.3 eV below the Fermi level. These features, common in CeX_c, have been clarified in detail by angle-resolved photoemission spectroscopy and de Haas–van Alphen effect measurements.[15–17]

In this work, we have measured the electrical resistivity of CeX_c under high pressures of up to 8 GPa to study the enhancement of the Kondo effect and the crossover from the magnetic ordering regime to the Fermi liquid regime. We show that the $\ln T$ behavior in the resistivity is enhanced by applying pressure in all the CeX_c compounds. The pressure dependences of T_N, CEF splitting, the coefficient of the $\ln T$ term, and the temperatures of the resistivity maximum below which the Fermi liquid state is formed, are extracted from the data. Although the overall feature can be understood in the framework of Doniach's diagram, we suggest that the level lowering of the Γ_8 excited state at high pressures gives rise to some distinct phenomena in CeX_c in the crossover region around the QCP. We compare these results with those of other intermetallic compounds.

2. Experiment

Single-crystalline samples were prepared by the Bridgman method as described in Ref. 16. Resistivity under high pressure was measured by the normal four-terminal method. The current direction was along the [001] axis. For measurements up to 2.5 GPa, we used a CuBe/NiCrAl hybrid-piston-cylinder cell with daphne oil as a pressure-transmitting medium. Magnetic field was also applied using a 15 T cryomagnet. The field direction was along the [001] axis, which was parallel to the current direction. Measurements up to 8 GPa were performed at zero field using a cubic anvil cell with fluorinert as a pressure-transmitting medium.

3. Experimental Results

3.1 Resistivity at zero field

3.1.1 CeTe

Figure 1(a) shows the temperature (T) dependences of the resistivity (ρ) of CeTe at several pressures. The $\rho(T)$ of LaTe is also shown for reference to estimate the contribution of phonon scattering. At ambient pressure, a hump anomaly is observed at around 20 K, reflecting CEF splitting; ρ decreases below ~ 20 K because magnetic scattering through the Γ_8 excited state gradually vanishes. We denote this characteristic temperature T^*. With further decrease in temperature, ρ drops steeply at 2 K, reflecting the AFM order. The $\ln T$ behavior in $\rho(T)$ due to the Kondo effect can be recognized above T^* after subtracting the $\rho(T)$ of LaTe, whereas it is not recognizable below T^*. These behaviors are consistent with a previous study.[8]

With increasing P, $\rho(T)$ exhibits a clear $\ln T$ dependence below ~ 100 K even before subtracting the $\rho(T)$ of LaTe. This shows that the Kondo effect (single-site Kondo scattering) is enhanced by pressure. If we subtract the $\rho(T)$ of LaTe, the $\ln T$ dependence continues up to 300 K. The hump anomaly at T^* shifts to lower temperatures, corresponding to the level lowering of the Γ_8 excited state.[12] However, above 2.5 GPa, the hump anomaly is no longer distinguishable from the peak emerging around 6 K, probably reflecting the Kondo coherence. We denote this temperature of resistivity maximum as T_{m1} hereafter. When P is increased from 3.5 to 5 GPa, the coherence peak slightly shifts to a higher temperature, which seems to reflect an increase in the Kondo temperature T_K. However, the peak unexpectedly shifts again to a lower temperature at 7.3 GPa, which is opposite to the normal P dependence of the coherence peak in Ce-based compounds. Although this could be somehow related to the transition to the CsCl structure at 8 GPa in CeTe,[18] the reason is unclear.

The low-temperature part of $\rho(T)$ at around T_N is shown in the inset of Fig. 2(a). As indicated by the arrows, the T_N of CeTe initially increases with increasing P and then starts to decrease above ~ 2 GPa. At 3.5 GPa, the anomaly in $\rho(T)$ corresponding to T_N can no longer be identified. The P dependence of T_N is plotted in Fig. 2(a). T_N determined from the specific heat measurement in Ref. 13 is also plotted. With respect to the successive transitions at 1.2 and 1.8 GPa reported in Ref. 13, the higher transition temperature is in agreement with T_N deduced from $\rho(T)$. No anomaly corresponding to the second transition at a lower temperature, which is indicated by the filled triangles in Fig. 2(a), was detected in $\rho(T)$ as a clear anomaly. The critical pressure P_c is estimated to be from 3 to 3.5 GPa, although this requires further study at lower temperatures.

3.1.2 CeSe

Figure 1(b) shows the $\rho(T)$ curves for CeSe up to 8 GPa. The $\rho(T)$ of LaSe is also shown for reference to estimate the contribution of phonon scattering. At ambient pressure, as in CeTe, the hump anomaly reflecting CEF splitting appears at around $T^* = 60$ K, and a kink anomaly due to the AFM order is clearly observed at 5.4 K. $\rho(T)$ weakly increases with decreasing T below ~ 20 K down to T_N. This increase can be ascribed to the Kondo effect within the Γ_7 ground state. The $\ln T$ behavior in the high-T region above T^* can be recognized after subtracting the $\rho(T)$ of LaSe. These behaviors at ambient pressure are consistent with a previous study.[8]

With increasing P, $\rho(T)$ increases and exhibits a clear $\ln T$ anomaly below ~ 200 K, which shows that the Kondo effect (single-site Kondo scattering) is enhanced by pressure. If we subtract the $\rho(T)$ of LaSe, the $\ln T$

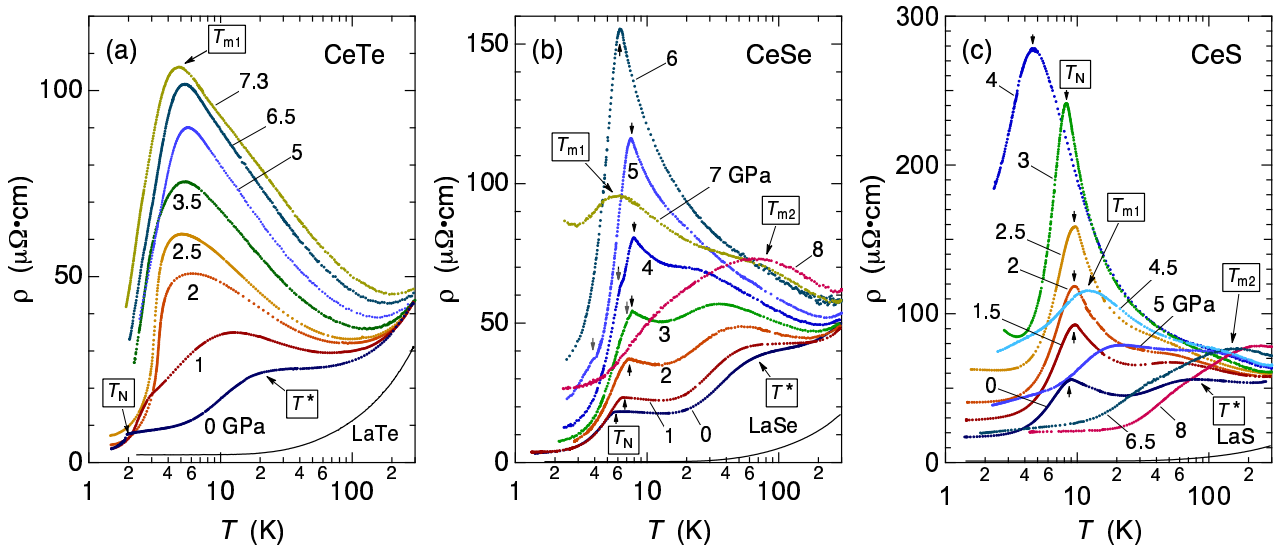

Fig. 1. (Color online) Temperature dependences of the electrical resistivities of (a) CeTe, (b) CeSe, and (c) CeS under high pressures. The resistivities of LaTe, LaSe, and LaS at ambient pressure are also shown for reference.

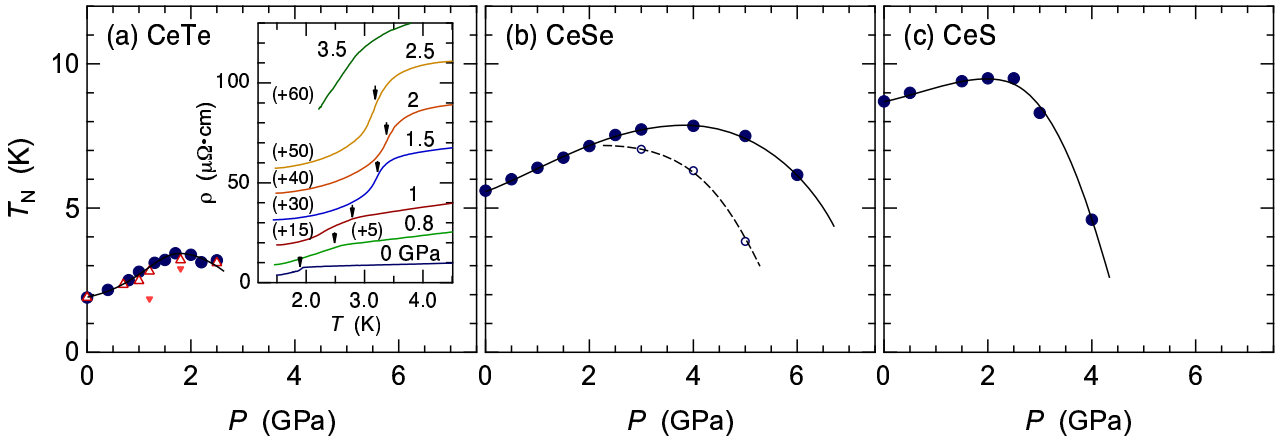

Fig. 2. (Color online) Pressure dependences of T_N of (a) CeTe, (b) CeSe, and (c) CeS, determined from $\rho(T)$ (open circles). The inset of (a) shows the $\rho(T)$ of CeTe in the vicinity of T_N. Open and filled triangles in (a) represent the transition temperatures of CeTe determined from the specific heat measurement in Ref. 13. The filled triangles at 1.2 and 1.8 GPa show the successive transitions. Open circles in (b) correspond to the weak anomalies observed in the $\rho(T)$ of CeSe below T_N.

dependence continues up to 300 K. Simultaneously, the hump anomaly at around T^* shifts to lower temperatures, indicating that the energy level of the Γ_8 excited state decreases with increasing P. Above 5 GPa, T^* is no longer recognizable because it is hidden behind the significant increase in $\rho(T)$ owing to the Kondo effect.

The $\ln T$ slope below ~ 20 K down to T_N, where the Kondo effect within the Γ_7 ground state dominates, also increases with P. Above 5 GPa, it is more enhanced and $\rho(T)$ exhibits a steep increase down to T_N, where a sharp cusp is observed. These behaviors are in contrast to those of CeTe at high pressures, where $\rho(T)$ follows a single $\ln T$ slope down to $T_{m1} \sim 6$ K and the cusp anomaly at T_N soon becomes unclear at high pressures above 2 GPa.

In CeSe, as indicated by the arrows in Fig. 1(b), T_N initially increases with P, taking a maximum at ~ 4 GPa, and decreases. The P dependence of T_N is plotted in Fig. 2(b). P_c is estimated to be around 7.5 GPa. Above 3 GPa, we can also see another weak anomaly in $\rho(T)$ below the main cusp anomaly at T_N, which is plotted by the open circles. We speculate that this transition reflects some change in the magnetic structure such as that discussed in CeTe by a mean-field calculation.[13] Namely, in the intermediate phase, the AFM moment is possibly oriented along the [100] axis because of the Γ_8 level lowering, and in the low-T phase the direction changes to the [111] axis, reflecting the easy axis of the Γ_7 ground state.

All these behaviors change significantly above 7 GPa, where $\rho(T)$ at low temperatures decreases significantly. At 7 GPa, a new broad peak appears at around 6 K, which we suggest as the peak of T_{m1}, the same kind of Kondo coherence peak as that observed in CeTe. The upturn in $\rho(T)$ below 3 K suggests the AFM ordering existing below the lowest temperature of 2.5 K. Also note that there is a broad hump anomaly at around 60 K, which we

denote T_{m2}. At 8 GPa, the position of this peak shifts to around 70 K, above which the $\ln T$ behavior is still observed. At low temperatures below 70 K, $\rho(T)$ shows a more significant decrease down to the lowest temperature, suggesting the formation of a Fermi liquid state. Therefore, the broad peak at T_{m2}, i.e., 60 K at 7 GPa and 70 K at 8 GPa, may also be assigned to another Kondo coherence peak. The coherence peak at T_{m1} still seems to exist at around 15 K, where a broad hump is observed. Thus, the double-peak structure in $\rho(T)$ is characteristic of CeSe in the Fermi liquid regime, and both T_{m1} and T_{m2} shift to higher temperatures with increasing P.

3.1.3 CeS

Figure 1(c) shows the $\rho(T)$ curves of CeS at high pressures. At ambient pressure, in the same way as in CeTe and CeSe, the hump anomaly reflecting CEF splitting appears at around $T^* = 70$ K, and a cusp anomaly due to the AFM order is clearly observed at 8.7 K. An increase in $\rho(T)$ with decreasing T is observed below ~ 20 K down to T_N, which can be ascribed to the Kondo effect within the Γ_7 ground state. The slope of the $\ln T$ dependence in the low-T region is larger than that of CeSe. The $\ln T$ dependence is also visible in the high-T region above T^* even before subtracting the $\rho(T)$ of LaS. The largest slopes of the $\ln T$ dependences in CeS at ambient pressure, in both the high- and low-T regions, show that c–f hybridization is strongest in CeS among the three compounds of CeX_c. These behaviors at ambient pressure are consistent with that observed in a previous study.[8)]

With increasing P, the $\ln T$ slope increases as in CeTe and CeSe, reflecting the enhancement of the Kondo effect (single-site Kondo scattering). A surprising phenomenon in CeS is that $\rho(T)$ in the low-T region increases more steeply than the $\ln T$ slope in the high-T region. This behavior becomes more significant above 2.5 GPa. The increase in $\rho(T)$ on approaching T_N, which can probably be ascribed to the enhancement of the Kondo effect, is much larger than that in CeSe. With respect to T_N, it initially increases with increasing P, followed by a maximum at around 2 GPa, and decreases to 4.5 K at 4 GPa. The upturn in $\rho(T)$ of 3 GPa below 3.5 K suggests another AFM ordering existing below the lowest temperature of 2.8 K. The P dependence of T_N is plotted in Fig. 2(c). P_c is estimated to be around 4.5 GPa.

Above 4.5 GPa, a significant change takes place at low temperatures. Although the $\ln T$ behavior remains at high temperatures above 100 K, $\rho(T)$ at low temperatures decreases significantly with increasing P. At 4.5 GPa, a new broad peak appears at around 12 K, which we suggest as the peak of T_{m1}, the same kind of Kondo coherence peak as those observed in CeTe and CeSe. Again note that there is another broad hump anomaly at around 100 K, which we denote T_{m2}. With further increase in P, these broad peaks shift to higher temperatures. Finally, at 8 GPa, the $\rho(T)$ curve becomes like that of a typical Fermi liquid system. However, the two broad peaks at T_{m1} and T_{m2} still remain in $\rho(T)$ at 8 GPa; one is at around 60 K and the other is at around 200 K, both of which may be ascribed to the coherence peak as in CeSe.

3.2 Magnetoresistance

Figure 3 shows the temperature dependences of electrical resistivity in magnetic fields and under high pressures for CeTe, CeSe, and CeS. All the compounds generally exhibit a negative magnetoresistance (MR). In CeTe, the MR effect increases significantly with increasing P. At 1.5 and 2.5 GPa, where the Kondo effect is clearly recognized in the $\ln T$ behavior in $\rho(T)$ at zero field, the ρ value decreases and the peak in $\rho(T)$ at T_{m1} shifts to higher temperatures with increasing field. This is a characteristic behavior observed in concentrated Kondo systems.[19,20)] In CeSe and CeS, by contrast, although the MR effect increases with increasing P, it is not so significant in comparison with that of CeTe. This is because the system is still well inside the magnetic ordering regime at these pressures below 2.5 GPa. The Kondo temperature T_K for the Γ_7 ground state may be much smaller than T_N. In CeTe, on the other hand, T_K is expected to be already larger than T_N at pressures of 1.5 and 2.5 GPa because of the high degeneracy of the ground state due to the almost collapsed CEF.[21,22)]

To describe the MR associated with the Kondo effect in more detail, we show in Fig. 4 the temperature dependences of the relative MR at 14.5 T for several pressures. We focus on the temperature range well above T_N: $T > 5$ K for CeTe and $T > 10$ K for CeSe and CeS. The magnitudes of MR in CeSe and CeS are almost the same. If we observe in detail, however, MR is almost independent of P below 2.5 GPa in CeSe, whereas in CeS MR increases slightly with increasing P.

Note that CeTe has the largest MR among the three compounds despite the fact that J_{cf} is the smallest. This may be because the f-state degeneracy affected by the low-lying Γ_8 excited level, which increases T_K, is the largest among the three compounds even at ambient pressure. With increasing P, the MR in CeTe increases below ~ 15 K, and it becomes almost independent of P above 1.5 GPa. Also note that the MR does not change with P above ~ 15 K.

Finally, we comment on the magnetic ordering. In CeTe, T_N exhibits a significant dependence both on the applied field and pressure, which can be explained by considering the magnetic and quadrupolar interactions in addition to the Γ_8 level lowering as we have shown in previous studies.[12,13)] In CeSe and CeS, by contrast, T_N is hardly affected by the field in this P range below 2.5 GPa. This is because the energy scale of the magnetic interaction is larger than that of CeTe, resulting in a larger T_N, and also because the Γ_8 level is still located at a high energy and therefore the level mixing does not affect the magnetic ordering. Finally, although this is not a subject of this work, weak anomalies observed in CeS below T_N in Fig. 3, which are clearly identified at 0 and 1.5 GPa in magnetic fields, reflect the change in the magnetic structure or domain distribution.[10)] We can also see this phase boundary in CeSe at 3.5 K in the data at 0 GPa and 10 T. This anomaly moves to $H < 10$ T at 1.5 and 2.5 GPa, which are not shown in Fig. 3.

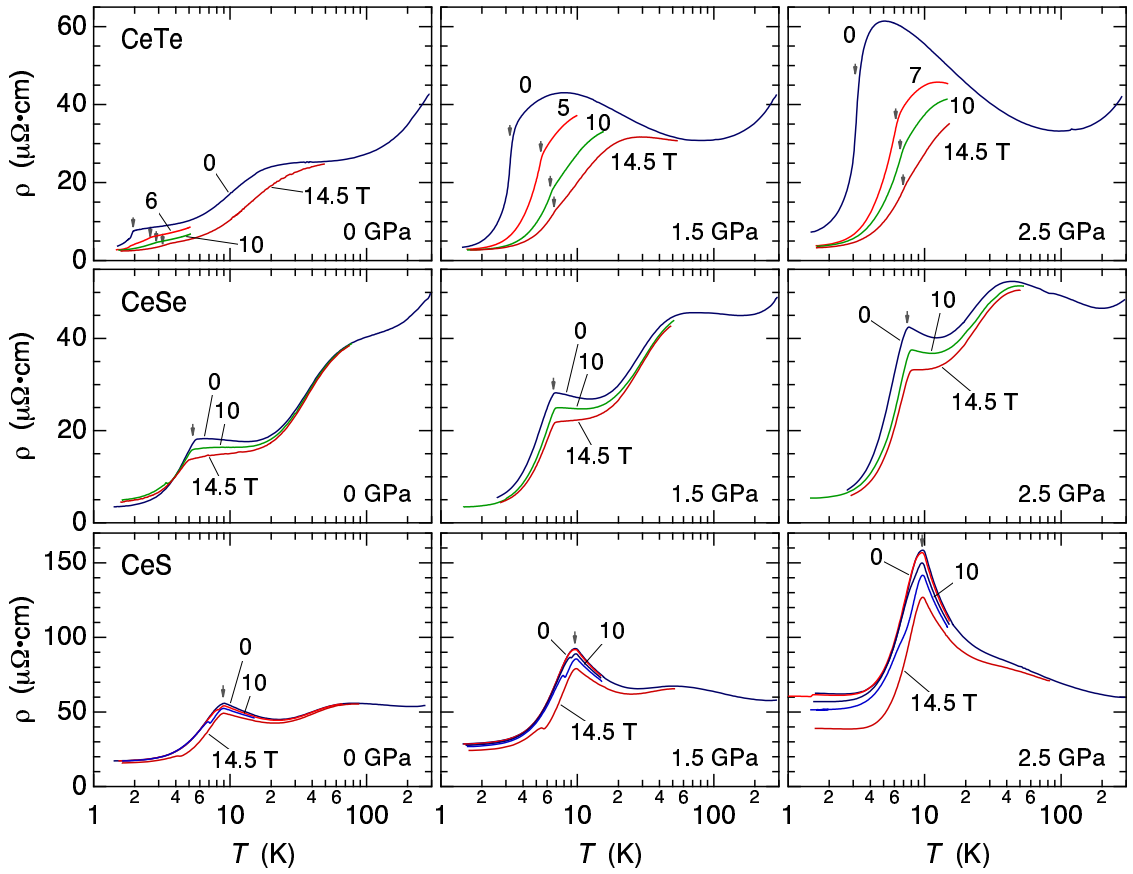

Fig. 3. (Color online) Temperature dependences of electrical resistivity in magnetic fields and under high pressures for CeTe, CeSe, and CeS. The arrows indicate the temperatures of antiferromagnetic ordering.

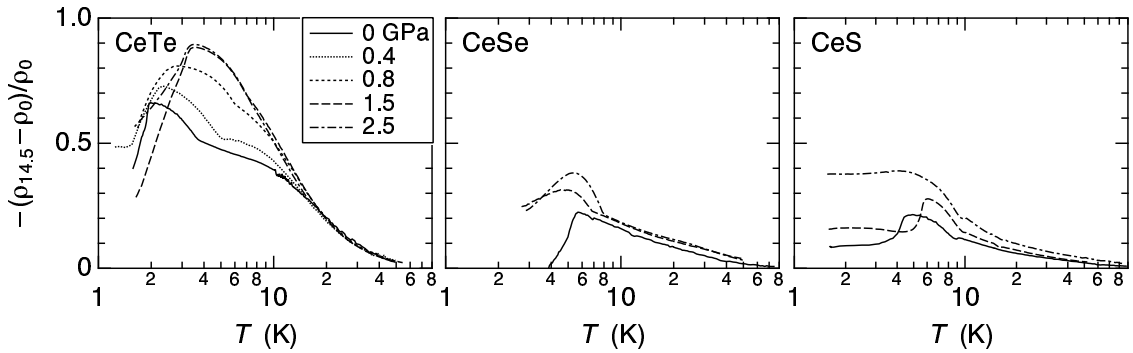

Fig. 4. Temperature dependences of the magnetoresistance at 14.5 T, $-(\rho_{14.5} - \rho_0)/\rho_0$, at several pressures.

4. Discussion

In Ce compounds, the coefficient of the $\ln T$ term in the magnetic part of the resistivity, $d\rho_{\rm mag}/d\ln T \equiv S$, is generally associated with $J_{cf}D(\varepsilon_F)$, where $D(\varepsilon_F)$ represents the density of states of sconduction electrons at the Fermi energy. When the system is in the magnetic ordering regime in Doniach's diagram, as in the present case of CeX_c, the coefficient S and ρ value at low temperatures generally increase with increasing P. In addition, in this regime, a double-peak structure is observed in $\rho_{\rm mag}(T)$ in many systems. The examples are $CeAl_2$, $CeCu_2$, $CeAu_2Si_2$, $CeNiGe_3$, $Ce_2Pd_3Si_5$, and $Ce_2Ni_3Ge_5$.[5,23–28] The peak at high temperatures is generally interpreted as reflecting the CEF level splitting of the f state and the second peak at low temperature as the formation of a coherent Kondo state. When the system is near the boundary between the magnetic ordering regime and the Fermi liquid regime, $\rho_{\rm mag}(T)$ generally exhibits a single peak at around the Kondo coherence temperature, and the peak shifts to high temperatures with increasing P without changing the peak height. The peak position can finally reach 300 K. The peak of CEF seems to merge with the coherence peak. The examples are $CeIn_3$, $CeAl_3$ and $CeCu_6$.[4,29–31] To discuss the pres-

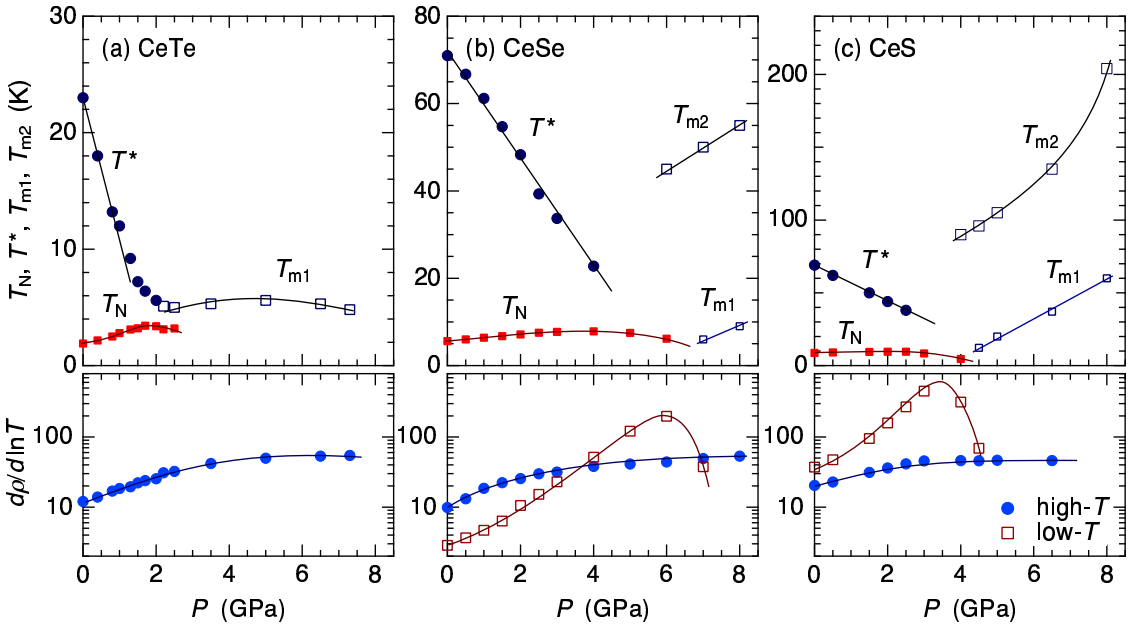

Fig. 5. (Color online) (Top panels) Pressure dependences of the characteristic temperatures T_N, T^*, T_{m1}, and T_{m2}. The lines are guides for the eye. It is remarked that all the three lines for T^* are expressed as $T^*(P) = T^*(0) - 12.2P$. (Bottom panels) Pressure dependences of the coefficient of the $\ln T$ term in the magnetic part of the resistivity, $d\rho_{mag}/d\ln T$, which are estimated in the high-T region above T^* or T_{m2} and in the low-T region between T_N and T^* or between T_{m1} and T_{m2}.

sure dependences of these characteristic temperatures of CeX_c, in Fig. 5 we plot T_N, T^*, T_{m1}, T_{m2}, and the slope S, which have been deduced from $\rho_{mag}(T)$, as functions of pressure. $\rho_{mag}(T)$ was obtained by subtracting the $\rho(T)$ of LaX_c. We discuss these parameters in the following. The most important and distinctive feature we consider in CeX_c is the shrinking of the CEF under pressure, which is reflected in the P dependence of T^*. This effect leads to the increase in the f-state degeneracy and, therefore, to the increase in T_K.[21,22]

First, we discuss the P dependence of the $\ln T$ term in $\rho(T)$. When the CEF anomaly at around T^* is at sufficiently high temperatures, we can extract two different coefficients of the $\ln T$ term from high-T and low-T regions above and below T^*, which we represent as S_H and S_L, respectively. The pressure dependences of these coefficients are also shown in the bottom panels of Fig. 5. In CeTe, since the peak at T^* soon merges with a peak at T_{m1}, only S_H is shown. In CeSe and CeS, the two regions are clearly separated up to P_c where T_N vanishes. With respect to the pressure dependence of S_H, they almost coincide with each other at high pressures, although the S_H for CeS is slightly larger than others at $P = 0$. We also see that the increasing rate of S_H with pressure is almost the same in CeX_c. On the other hand, the S_L for CeS is almost ten times larger than that for CeSe. The S_L for CeTe cannot be recognized, which is probably because the Kondo scattering in CeTe is too small and hidden behind the magnetic scattering due to disordered moments. This difference in S_L shows that the Kondo effect in the low-T region within the Γ_7 ground state is strongest in CeS and weakest in CeTe. By contrast, the similar S_H values suggest that the Kondo effect in the high-T region is more affected by the f-state degeneracy involving all the CEF states than the c–f hybridization effect.

Another point to be noted is that S_L exceeds S_H in CeSe and CeS at high pressures. Theoretically, the $\ln T$ coefficient is associated with the degeneracy λ of the f state and is proportional to $\lambda^2 - 1$.[32] In the high-T region, $\lambda = 6$, and in the low-T region when only the Γ_7 ground state is thermally populated, $\lambda = 2$. Therefore, S_H is generally larger than S_L, which is actually the case in many other intermetallic compounds.[5,23] In this sense, CeSe at low pressures is normal. Although the larger increasing rate of dS_L/dP than of dS_H/dP is also observed in $CeAl_2$,[23] it is particularly anomalous in CeSe and CeS that S_L exceeds S_H.

Next, with respect to T_N, T^*, T_{m1}, and T_{m2}, a general behavior observed in other inter-metallic compounds in the magnetic ordering regime can be summarized as follows (see Fig. 3 in Ref. 5 or Fig. 2 in Ref. 23):

(1) Double peaks appear at T^* and T_{m1} ($T^* > T_{m1}$). With increasing P, T^* slightly decreases and T_{m1} slightly increases.

(2) At around P_c, T_{m1} starts to increase rapidly and merges with T^*. Then, a single peak remains in $\rho(T)$ and T^* is renamed as T_{m2}, below which the Fermi liquid state is formed.

(3) T_{m2} increases with increasing P.

These behaviors are actually reproduced by a theory including the CEF effect.[33] However, the behaviors of these characteristic temperatures in CeX_c are slightly different:

(1) T^* decreases with increasing P much more rapidly

at a rate of −12.2 K/GPa.

(2) T^* and T_{m2} appear not to be connected in CeSe or CeS. A double-peak structure is still observed above P_c.

The slight decrease in T^* with P in general cases means that the true CEF level does not actually change with P. In the present cases of CeX_c, however, the rapid decrease in T^* with P seems to show that the actual CEF splitting decreases with P.[12,13] This is the most important and distinctive feature we consider in CeX_c, which is associated with the f-state degeneracy and the increase in T_K. This effect might also be associated with the anomalous increase in S_L at high pressures.

P_c could also be affected by the pressure-dependent CEF splitting. From Fig. 2, we see that P_c is largest in CeSe and lowest in CeTe. Although the P dependence of T_N of CeX_c follows that of Doniach's diagram, this sequence of P_c does not coincide with that of the strength of J_{cf}, which is smallest in CeTe and largest in CeS. Here, it is necessary to take into account the difference in CEF splitting, i.e., it is largest in CeS and smallest in CeTe. Particularly in CeTe, CEF splitting soon vanishes at around 2 GPa, where T_N starts to decrease. The smallest P_c in CeTe can be understood by considering the increased degeneracy of the f state owing to the collapsed CEF, which results in more significant increase in T_K compared with those in CeSe and CeS. Then, the T_N of CeTe vanishes at the smallest pressure among the three compounds.

We consider that the pressure dependence of T_N in Fig. 2 can be understood as a result of three effects. Firstly, with increasing P, J_{cf} increases, which results in the enhancement of the RKKY interaction and T_N. Secondly, the Γ_8 CEF level decreases, which also contributes to the increase in T_N because the Γ_8 state can give rise to a larger magnetic moment. This is explained in Ref. 13 for CeTe by a mean-field model calculation. Both these effects contribute to the increase in T_N. Thirdly, T_K increases with P through the increase in both J_{cf} and the f-state degeneracy. In the present case of CeX_c, we suggest that the latter effect affects T_K more than J_{cf}.

The MR effect can also be roughly explained. In CeSe and CeS below 2.5 GPa, the Γ_8 state is still well separated and the MR effect reflects the suppression of the Kondo effect within the Γ_7 ground state by the applied field. To understand the weak MR effects in CeSe and CeS shown in Fig. 4, Fig. 2 in Ref. 20 based on a periodic Anderson model is a good reference. With increasing P, the T_K of the Γ_7 ground state increases, and the scaled parameters of T/T_K and H/T_K decrease. Since we are in the region of $T/T_K > 1$, the increase in MR caused by the decrease in T/T_K would be cancelled by the decrease in H/T_K. Then, the MR effect is expected to be weak in CeSe and CeS. To understand in more detail the larger P dependence of MR in CeS than in CeSe, it is necessary to consider that J_{cf} is larger in CeS than in CeSe (see S_L in Fig. 5) and that the pressure region of 0 – 2.5 GPa in CeS is closer to P_c, or the pressure where S_L takes the maximum value. It is also necessary to take into account the gradual increase in the f state degeneracy at high pressures.

The much larger MR effect in CeTe should be more related to the higher degeneracy owing to the small CEF splitting, which almost vanishes above 1.5 GPa. Although J_{cf} is smallest in CeTe among the three compounds, the larger degeneracy of the f-state enhances the Kondo effect and leads to a large MR effect. Note that, in Fig. 4, the MR of CeTe increases with P up to 1.5 GPa and becomes almost independent of P above 1.5 GPa. This coincides with the shrinking of CEF, which is demonstrated by the variation in T^* in Fig. 5(a). Above 1.5 GPa, the degeneracy of the ground state does not increase any further with P, and then the MR effect hardly changes with P, which may be explained in the same way as in CeSe and CeS by the decrease in T/T_K and H/T_K. Above 15 K, where the Γ_8 excited level is well populated, the f-state can be recognized as being fully degenerate, and the MR shows little P dependence.

Finally, although we have studied a wide region of pressure, temperature, and magnetic field space, note that there still remains a low-temperature region below 2 K that should be studied in the future. As shown by the $\rho(T)$ curves in Fig. 1, the ρ values at 2 K are still much higher than the residual resistivities, which are expected from the extrapolation of the $\rho(T)$ curves at 0 GPa. This shows that the system has not yet reached to the ground state, especially near pressures at around P_c, and there remains a possibility that some drastic phenomena occur below 2 K.

5. Conclusions

We have studied the Kondo effect in CeS, CeSe, and CeTe by electrical resistivity measurements under high pressures of up to 8 GPa. The $\ln T$ term in the temperature dependence of the resistivity commonly increases with increasing pressure, indicating that c–f hybridization is enhanced by pressure. There are two $\ln T$ regions. One is at high temperatures, where both Γ_7 and Γ_8 states are involved, and the other is at low temperatures, where the Γ_7 ground state is mainly involved, resulting in the peak structure in $\rho(T)$ at around T^* reflecting CEF splitting. From the $\ln T$ term in the low-temperature region, we see that J_{cf} is largest in CeS and smallest in CeTe.

CeX_c under high pressure starts from the magnetic ordering regime and the pressure dependence of T_N can basically be understood from Doniach's diagram. However, it is necessary to take into account the significant decrease and collapse of CEF splitting under pressure to interpret the sequence of P_c, where T_N vanishes; $P_c(\mathrm{CeTe}) < P_c(\mathrm{CeS}) < P_c(\mathrm{CeSe})$, which contradicts with the sequence of J_{cf}. We suggest that the increase in T_K under high pressure, which is brought about more by the increase in the f-state degeneracy than by the increase in J_{cf}, is responsible for the pressure dependence of T_N and magnetoresistance.

Finally, the appearance of the double-peak structure in $\rho(T)$ in CeSe and CeS at high pressures near and above P_c is also a distinctive feature of CeX_c. Since T^* seems to be connected to the low-temperature peak at T_{m1}, the second peak at T_{m2} suggest the appearance of another

energy scale associated with the formation of the Kondo singlet state. In any case, however, this remains an open question to be studied in the future.

Acknowledgements

This work was carried out by a joint research in the Institute for Solid State Physics, The University of Tokyo, and was supported by JSPS KAKENHI Grant Numbers 2430087 and 15K05175.

1) S. Doniach, Physica B+C **91**, 231 (1977).
2) J. Otsuki, H. Kusunose, and Y. Kuramoto, J. Phys. Soc. Jpn. **78**, 034719 (2009).
3) H. v. Löhneysen, A. Rosch, M. Vojta, and P. Wölfle, Rev. Mod. Phys. **79**, 1015 (2007).
4) G. Knebel, D. Braithwaite, P. C. Canfield, G. Lapertot, and J. Flouquet, Phys. Rev. B **65**, 024425 (2001).
5) Z. Ren, L. V. Pourovskii, G. Giriat, G. Lapertot, A. Georges, and D. Jaccard, Phys. Rev. X **4**, 031055 (2014).
6) F. Hulliger, B. Natterer, and H. R. Ott, J. Magn. Magn. Mater. **8**, 87 (1978).
7) H. R. Ott, J. K. Kjems, and F. Hulliger, Phys. Rev. Lett. **42**, 1378 (1979).
8) J. Schoenes and F. Hulliger, J. Magn. Magn. Mater. **63&64**, 43 (1987).
9) J. Rossat-Mignod, J. M. Effantin, P. Burlet, T. Chattopadhyay, L. P. Regnault, H. Bartholin, C. Vettier, O. Vogt, D. Ravot, and J. C. Achart, J. Magn. Magn. Mater. **52**, 111 (1985).
10) A. Dönni, A. Furrer, P. Fisher, S. M. Hayden, F. Hulliger, and T. Suzuki, J. Phys: Condens. Matter **5**, 1119 (1993).
11) A. Dönni, A. Furrer, P. Fisher, and F. Hulliger, Physica B **186-188**, 541 (1993).
12) Y. Kawarasaki, T. Matsumura, M. Sera, and A. Ochiai, J. Phys. Soc. Jpn. **80**, 023713 (2011).
13) H. Takaguchi, Y. Hayashi, T. Matsumura, K. Umeo, M. Sera, and A. Ochiai, J. Phys. Soc. Jpn. **84**, 044708 (2015).
14) K. Matsubayashi, T. Tanaka, A. Sakai, S. Nakatsuji, Y. Kubo, and Y. Uwatoko, Phys. Rev. Lett. **109**, 187004 (2012).
15) M. Nakayama, H. Aoki, A. Ochiai, T. Ito, H. Kumigashira, T. Takahashi, and H. Harima, Phys. Rev. B **69**, 155116 (2004).
16) M. Nakayama, N. Kimura, H. Aoki, A. Ochiai, C. Terakura, T. Terashima, and S. Uji, Phys. Rev. B **70**, 054421 (2004).
17) G. Chiaia, L. Duò, O. Tjernberg, M. Göthelid, M. Björkqvist, H. Kumigashira, S.-H. Yang, T. Takahashi, T. Suzuki, and I. Lindau, Phys. Rev. B **57**, 12030 (1998).
18) J. M. Leger, R. Epain, J. Loriers, D. Ravot, and J. Rossat-Mignod, Phys. Rev. B **28**, 7125 (1983).
19) A. Takase, K. Kojima, T. Komatsubara, and T. Kasuya, Solid State Commun. **36**, 461 (1980).
20) N. Kawakami and A. Okiji, J. Phys. Soc. Jpn. **55**, 2114 (1986).
21) K. Yamada, K. Yosida, and K. Hanzawa, Prog. Theor. Phys. **71**, 450 (1984).
22) K. Hanzawa, K. Yamada, and K. Yosida, J. Magn. Magn. Mater. **47&48**, 357 (1985).
23) H. Miyagawa, G. Oomi, M. Ohashi, I. Satoh, T. Komatsubara, M. Hedo, and Y. Uwatoko, Phys. Rev. B **78**, 064403 (2008).
24) E. Vargoz, P. Link, D. Jaccard, T. Le Bihan, and S. Heathman, Physica B **229**, 225 (1997).
25) P. Link and D. Jaccard, Physica B **230**, 31 (1997).
26) M. Nakashima, K. Tabata, A. Thamizhavel, T. C. Kobayashi, M. Hedo, Y. Uwatoko, K. Shimizu, R. Settai, and Y. Ōnuki, J. Phys: Condens. Matter **16**, L255 (2004).
27) N. Kurita, H. Yamamoto, M. Hedo, T. Fujiwara, T. Shigeoka, S. W. Tozer, and Y. Uwatoko, Physica B **403**, 1479 (2008).
28) M. Nakashima, H. Kohara, A. Thamizhavel, T. D. Matsuda, Y. Haga, M. Hedo, Y. Uwatoko, R. Settai, and Y. Ōnuki, J. Phys: Condens. Matter **17**, 4539 (2005).
29) T. Kagayama, T. Ishii, and G. Oomi, J. Alloys Compds. **207-208**, 263 (1994).
30) G. Oomi and T. Kagayama, J. Phys. Soc. Jpn. **65**, 2732 (1996).
31) S. Raymond and D. Jaccard, J. Low Temp. Phys. **120**, 107 (2000).
32) B. Cornut and B. Coqblin, Phys. Rev. B **5**, 4541 (1972).
33) Y. Nishida, A. Tsuruta, and K. Miyake, J. Phys. Soc. Jpn. **75**, 064706 (2006).